Spatial-Pattern-Induced Evolution of a Self-Replicating Loop Network

Keisuke Suzuki*
Takashi Ikegami
Department of General Systems Sciences
The Graduate School of Arts and Sciences
University of Tokyo
3-8-1 Komaba
Tokyo 153-8902, Japan
ksk@sacral.c.u-tokyo.ac.jp
ikeg@sacral.c.u-tokyo.ac.jp

Abstract We study a system of self-replicating loops in which interaction rules between individuals allow competition that leads to the formation of a hypercycle-like network. The main feature of the model is the multiple layers of interaction between loops, which lead to both global spatial patterns and local replication. The network of loops manifests itself as a spiral structure from which new kinds of self-replicating loops emerge at the boundaries between different species. In these regions, larger and more complex self-replicating loops live for longer periods of time, managing to self-replicate in spite of their slower replication. Of particular interest is how micro-scale interactions between replicators lead to macro-scale spatial pattern formation, and how these macro-scale patterns in turn perturb the micro-scale replication dynamics.

Keywords
Self-replication, cellular automata, evolution, hypercycle, evoloop

1 Introduction

Open-ended evolution is one of the challenging problems of artificial life studies [1]. It is simply defined as the continuing generation by evolutionary systems of novel phenotypic characteristics. In particular, the necessary conditions for open-ended evolution remain to be understood.

Unfortunately, only a few examples of open-ended evolution are available, such as open-endedness in forms, (e.g., [20, 8]) and in programs (e.g., [4, 12, 7, 10]). One of the earliest examples is Lindgren's model of evolutionary game dynamics. He showed that the memory strategies of the iterated prisoner's dilemma game lead to continuous growth of memory size. Such growth is supported by the duplication dynamics of binary strings that encode a game strategy [10]. Sims' artificial creatures give another example of evolution of diversified forms. The underlying mechanism can be thought as a mixture of physical embodiment and internal logical circuitry [20]. These two examples certainly show increasing complexity of replicating systems, but whether they are truly open-ended or not is still unknown. This is also true for the Tierra system of artificial creatures.

We focus on the open-ended properties of a simple replicating system. In particular, we study an extension of Langton's loops (e.g., [22, 9, 6, 21, 11, 3, 17]) to explore the properties of open-ended evolution. Langton's original loop lacks a universal capability for replicating forms. Morita and Imai designed a new loop model that has such a universal capability. Tempesti also extended Langton's model to make it universal. But from the point of view of open-ended evolution, the interactions between loops are important and need to be investigated. Sayama designed a new replicating loop

* Corresponding author.

system [17], where collisions between loops generated novel species, which is a first step in this direction. In Sayama's earlier work, the size of loops was found to gradually decrease on average, and thus they cannot exhibit open-ended evolution. Further investigations showed that certain loop configurations *can* sustain and develop complexity of the loops [13, 14].

We extend these studies by introducing a food-web structure between loops. For the basic model, we extended Sayama's shape-encoding worm system [18] to make it a universal replicator. Species are simply distinguished by an extra tag, and the transition rules may be a function of such additional *species bits*. Those with the same tag have no way of distinguishing whether objects undergoing replication are part of their own structure or that of another replicator. The distinction between organism and environment is thus blurred, enabling replicators to mutate and create novel structural variants. As a result, spatiotemporal patterns constructed by the loops can lead to new types of loops.

Our simulation results yield two observations. Firstly, we report the micro dynamics by which new replicators emerge. Some statistical analysis shows that there are four micro-mutation types, and the mutation event caused by fusion processes among loops is the most frequently observed. Secondly, we show that populations of self-replicating loops can generate macro-scale spatial patterns, such as spirals, that are distinct from the micro-scale behavior of the individual replicators themselves. Larger loops with longer life spans emerge and breed locally at the boundary regions between different species in these spiral formations.

In Section 2, we introduce the design of the present model. The assumed food-web structure is detailed in Section 3, and we study the effect of mutations in Section 4. The relationship between macroscopic structures and micro-level mutations is discussed in Section 5.

2 Model

There are two main aspects of the design in our model: the design of the self-replicating patterns themselves, and the interactions between them. We use a shape-encoding method originally introduced by Morita and Imai [11] to design a program of self-replicating loops. In their model, the self-replicating patterns' genetic information encodes their own shapes. Sayama introduced a variant of such a shape-encoding self-replicator, a *worm*, introducing interactions among replicators. Our self-replicating structure follows Sayama's "shape-encoding worm," but the rules that govern the process of self-replication are new.

Also, we introduce interactions between replicators. In Sayama's evoloop system, the dissolving loop resulting from the interaction leads to natural selection related to their replication rates. We designed several types of dissolving interactions between replicators to construct food-web networks. Such ecological relationships, which have not been studied in self-replicating cellular automata (CAs), can exhibit interesting relationships between global and local behaviors.

We now describe the model in terms of its (i) cell states, (ii) self-replication mechanisms, and (iii) interaction mechanisms.

2.1 Description of Cell States and Functional Roles

To aid intuition we use biological terminology throughout. However, we have the following definitions. A *cell* is defined as a minimal square in the two-dimensional space. A *loop* is a spatial entity specified by the connected cell states. A *gene* represents the shape of a loop that is given by a set of `gene` fields of the connected cells. A *species* is a special state value of the cell. The cells with different species indexes don't communicate with each other, so that a set of cells that constitutes a loop has a common species index. As a result, a loop is now characterized by the shape and the species index, and the loop-loop interaction can be twofold: interspecific and intraspecific.

Using this terminology, we give a detailed instruction of the CA rule. Each cell takes $128n + 1$ different possible states, where n specifies the number of species; each species identifies a way of response when interacting with other cells of the same or a different species (see Section 2.3). There is a unique `quiescent` (inactive) cell state that constitutes the background state. The remaining $128n$

states constitute structure states, and they are classified into three main fields according to their functional roles (Figure 1). We can independently design and execute the three fields, so that it is easy to designate a transition rule for self-replication dynamics.

Details of the three fields and one `species` field are given in Table 1. The `link` field constitutes a phenotypic structure (shape) of the organism that determines the path where genetic signals (genes) propagate. The gene field stores directional information (C, R, L) that is later translated into the direction of `link` fields in newly created cells. Finally, the `mode` field identifies the current functional role of a cell in the context of a self-replication process. In Table 2, each functional role associated with the `mode` fields is summarized briefly.

2.2 Self-replication Cycle

In what follows, rather than describing each state transition rule in detail, we instead outline a single self-replication cycle. The complete cycle is given in Appendix 1.

A self-replicator in our model is represented as a closed loop structure of connected `structure` cells. The directions of the `link` fields determine the connectivity between cells. The loop's shape is defined by the sequential values in `link` fields of cells constituting a loop.

The `gene` field in one cell stores information about the direction to take in creating a new cell in constructing a new loop structure (L, C, or R). The entire self-replication process is directed by the shape information coded in the `gene` fields (e.g., CLCLCLC) of all connected cells.

In contrast to Langton's SR loop [9], shape information is generated dynamically during the replication process. When phenotypic changes occur, the corresponding shape information is also automatically altered. Then the self-replication continues according to the new genetic information. Therefore, self-replicators are easier to be modify stably, which may lead to an increase in structural complexity. Each step of the self-replication cycle (encoding and propagation of genes, construction of new cells) is governed by the status of the `mode` field. At the beginning of the self-replication process, one cell is in the EXPLORE mode and all others are in the NORMAL mode.

Cells that have different values in their `species` field cannot constitute a same loop structure, because they do not interact with each other except in special cases (as will be discussed later in this article). During a normal self-replication cycle, all the cells forming one loop structure are thus assured of having the same values in the `species` fields.

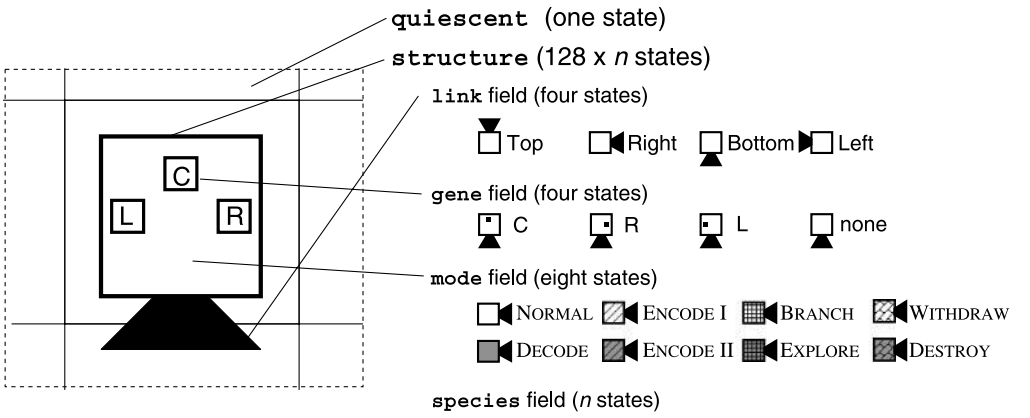

Figure 1. An illustration of cell states, classified into four different fields according to functional roles. The link field (four states) specifies cell direction (drawn as a black trapezoid). The gene field (four states) stores shape information for constructing new loop structures (drawn as a square in one of three locations). The mode field (eight states) stores special functional information to be used in the self-replication process (drawn as the fill patterns of the squares). The species field stores an index that identifies which interaction rules to use (drawn as the color of loops in selected figures; see, e.g., Figure 4). The design of the cell is based on the "shape-encoding worm" created and studied by Sayama [18].

Table 1. Roles of the four different fields that together describe each multilayered state. For a detailed description of the mode field, see Table 2.

Fields	No.	Name	Role
`link`	4	TOP, BOTTOM, RIGHT, LEFT	Specifies the direction of propagation of genes through the cell.
`gene`	4	C, R, L, none	Stores genetic information that is translated into the shape of the new loop structure.
`mode`	4	NORMAL, DECODE, ENCODE I, ENCODE II, BRANCH, EXPLORE, WITHDRAW, DESTROY	Describes the functional mode (see Table 2).
`species`	n	$S_1, S_2, \ldots S_n$	Identifies the species, which determines the appropriate interaction rules (see Section 2.3).

In Figure 2, the four processes constituting a normal self-replication cycle are shown: *corner positioning*, *shape encoding*, *arm extension*, and *arm withdrawal*. Note that, with the exception of arm withdrawal, these processes work in parallel in time and occur concurrently at the various stages of the self-replication cycle.

Corner positioning (t=0–3). This phase commences the self-replication cycle. The configuration of the parent loop consists of one cell in EXPLORE mode and all others in NORMAL mode. The EXPLORE mode is transferred counterclockwise through neighboring cells until it reaches the branch corner, where it switches to DECODE mode in preparation for the arm extension phase (Figure 2, t=2). The cell in DECODE mode then switches to BRANCH mode, a new cell is created in the arm, and its counterclockwise neighbor switches to ENCODE I mode, triggering the shape encoding phase (Figure 2, t=3).

Shape encoding (t=3–13). This phase is initiated with the last step of the corner positioning phase, at which point an ENCODE I mode cell has just been created next to the BRANCH mode

Table 2. Functions of the different mode fields.

Mode name	Functions
NORMAL	Propagates genetic information towards the leading cell.
DECODE	Translates genetic information into new cells at the end of the arm.
ENCODE I ENCODE II	Encodes the direction of the leading cell.
BRANCH	Marks the starting point from which the arm extends.
EXPLORE	Cycles around the loop until reaching the branching corner.
WITHDRAW	Destroys all `structure` cells not in the BRANCH mode.
DESTROY	Destroys all `structure` cells (structural dissolution).

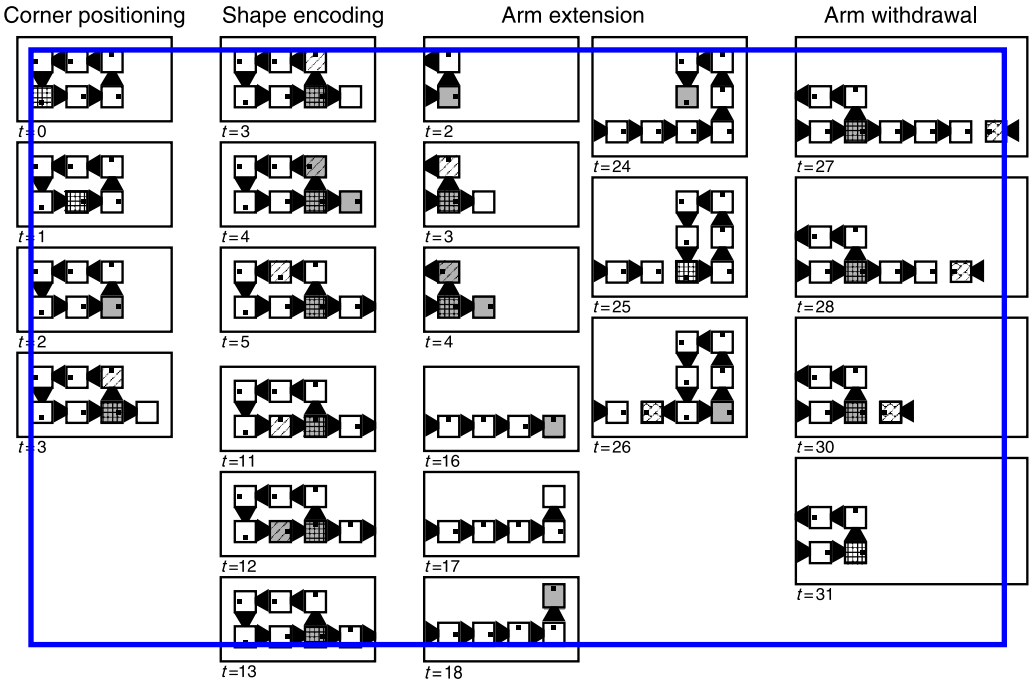

Figure 2. Self-replication mechanisms of a six-cell loop. Replication of arbitrary loop structures proceeds by the same basic steps. For the meaning of each symbol refer to Figure 1.

cell (Figure 2, t=3). The ENCODE I mode cell switches to the ENCODE II mode cell, storing a connecting direction to the next cell into the gene field (Figure 2, t=4). Then, a new ENCODE I mode cell is created next to the ENCODE II mode cell (Figure 2, t=5). This process of alternating between two encode modes is propagated counterclockwise around the loop, encoding the phenotypic structure of the whole loop (connectivity of `link` field values) into the `gene` fields of the encode-mode cell; these field values are then propagated forward through the neighboring cells. The replicator's shape information is thus stored throughout the loop structure, in the propagating values stored in `gene` fields. For example, in Figure 2 (t=11), the shape information is read as CLLCCCC. At the corner BRANCH mode cell, the encoded shape information is propagated into the extending arm (see "Arm extension" below). Genes reentering the loop structure from the branch, however, are reset to the C gene. This is done to assure that, prior to the propagation of shape information, an arm of the sufficient length must be constructed, preventing collisions between parent and daughter loops (see "Arm extension" below).

Arm extension (t=2–26). This phase is initiated with the creation of a DECODE mode cell at the corner of the parent loop (Figure 2, t=3). Shape information encoded in the `gene` field values of cells is propagated through the corner BRANCH mode cell into the extending arm. When the gene information reaches the DECODE mode cell at the tip of the arm (Figure 2, t=16), this information is translated into a new loop structure (a new cell in the NORMAL mode oriented in the direction specified by the gene: Figure 2, t=17). In the next time step, this cell in NORMAL mode switches to DECODE mode, and the process is repeated (Figure 2, t=18). Construction of the new loop is completed when the tip of the arm encounters an earlier portion of its own structure (Figure 2, t=24), at which point the arm is cut to create a separate daughter loop. The cell connecting the parent to the daughter loop switches to EXPLORE mode, initiating the corner positioning phase in the daughter loop (Figure 2, t=25). This EXPLORE mode changes the tip of the parent loop to WITHDRAW mode in preparation

for the arm withdrawal phase (Figure 2, t=26). In a normal (unperturbed) self-replication cycle, the daughter loop inherits the same structure as that of the parent loop.

Arm withdrawal (t=27–31). This phase begins when the daughter loop is completed, and does not overlap in time with the other phases discussed above. Withdrawal of the arm begins when the tip of the arm of the parent loop switches to WITHDRAW mode (Figure 2, t=26). The effect of this mode is to sequentially remove cells of the extended arm, stopping only when it reaches the first corner cell (Figure 2, t=30). When it reaches this cell, it switches the corner BRANCH mode state into EXPLORE mode, initiating the next corner positioning phase in the parent loop (Figure 2, t=31).

We didn't mention the role of the DESTROY mode. This last mode is used only for implementing the interaction process between different species. We come back to the process in the next subsection.

2.3 Competitive Interaction Process

The self-replication process described in the last section works correctly when there is only a single loop in the CA space. However, with other loops competing for space to self-replicate, local intercellular interactions become critical. Following the Evoloop modeling approach, we classified the interaction types according to the idea of *structural dissolution* discussed and implemented by Sayama [15, 16]. Structural dissolution is one aspect of "death of life." It enables damaged organisms not just to stop their function like a crystal, but to dissolve to make space for healthy organisms. He introduced an extra state into Langton's original loop system for dissolution of damaged loops.

For structural dissolution, we use the DESTROY mode, which is not used in the basic self-replicating mechanisms described in the last subsection. This DESTROY mode only emerges at sites where collisions occur between neighboring loops. Unlike WITHDRAW mode, which only dissolves cells of the loop arm, DESTROY mode dissolves any of the cell types that constitute the basic loop structure.

We used a food-web structure to organize loop species according to their interactions with other species. These interactions, which decide the relative "superiority" or "inferiority" of competing species, together constitute a hypercycle-like network as shown in Figure 3. There are four basic types of interaction in this network:

Inroad. When the expanding arm of one loop collides with any part of the other loop, the first loop destroys the second loop, and the arm continues extending.

Counter. When the expanding arm of one loop collides with any part of the other loop, the first loop is destroyed, but the second loop is unaffected by the collision.

Defensive. When the expanding arm of one loop collides with any part of the other loop, the first loop retracts its extending arm, leaving the second loop unaffected by the collision. The two loops may thus coexist.

Cancel. When the expanding arm of one loop collides with the other loop, both loops are destroyed.

Examples of these four types of interaction are illustrated in Figure 3. The complete state transition table is given in Appendix 2. Note that genes are lost in the inroad interactions, because the decoding process of the left-hand loop is disturbed by the cells of the right-hand loop that are undergoing structural dissolution.

With these four interactions, a cycle of competitive relationships can be designed between multiple species. For example, the species S_2 is made superior to S_1 but inferior to S_3 by using the inroad interaction between S_2 and S_1 and the counter interaction between S_2 and S_3. Interactions between loops of the same species are made to be symbiotic by using the defensive interaction, which leaves both loops unaffected by the collision. The remaining interaction between species, which we call the cancel interaction, is symmetric: it destroys both loops in the collision (Figure 3).

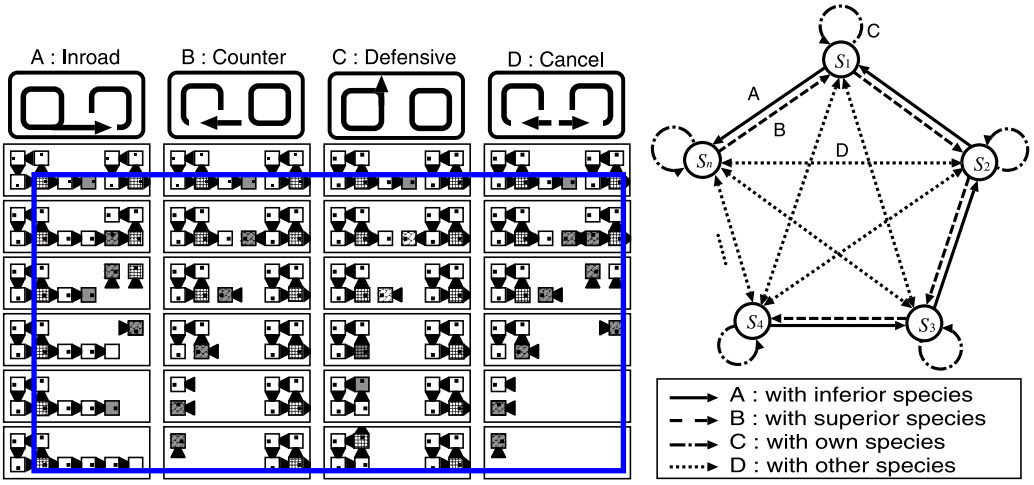

Figure 3. Relative strengths of the four different interaction types are illustrated in the collision processes depicted on the left. When the arm of a loop on the left side collides with a loop on the right, only the right-hand loop is destroyed by an inroad interaction, only the left loop is destroyed by a counter interaction, both of them survive following a defensive interaction, and both of them are destroyed following a cancel interaction. Competitive interaction-based relationships between species are illustrated in the food web shown on the right. Each species has exactly one superior and exactly one inferior species.

In collisions between the arm of one loop and any part of another loop, there is only one special case in which the above rules are not used. As mentioned in Section 2.2, the head of the construction arm encounters its own structure when the construction process of the daughter loop is reaching completion (arm bonding). Simply applying the above defensive rule to this case would thus disable the self-replication process. We therefore distinguish between two types of interaction in the case where cells of the same species index and of different species indexes collide with each other. When cells of the same species index come together, the collision of a constructing arm with another arm from the left-hand side is identified as the arm-bonding step of the self-replication process and is therefore allowed to occur. When cells of different species index collide, we apply the defensive rule so that the extending arm is withdrawn.

The structure of interactions between different species described above allows a variety of different self-replicators to coexist in the CA space. Dynamics of this kind have not been studied in the previous CA models of self-replicators, and will be the focus of this article.

3 Spatiotemporal Pattern of a Loop Ensemble

We study a simple food-web structure, that is, a hypercycle type of the linear case; that is, the network is expressed as $S_1 \rightarrow S_2 \rightarrow \cdots \rightarrow S_{n-1} \rightarrow S_n \rightarrow S_1$. It should be noted here that those different interaction types are defined between cell sites, not between loop units.

As visualized in Figure 4, the spatial region of S_i is invaded by that of S_{i+1} and in turn invades that of S_{i-1}. This chain relationship generates a spiral or strip waveform from most initial configurations. Generally, the pattern fluctuates between spiral and strip patterns.

In the upper series of snapshots of Figure 4, the dynamics of a system of five species is shown. The initial configuration of this system consists of loops of length 4, randomly distributed in the periodic domain. Different colors in these snapshots denote different species. The white species overwhelms the black species, the black species overwhelms the gray species, and so on [in the grayscale bar at the base of each snapshot, the order of colors goes from inferior (left-hand side) to superior (right-hand side)]. The center of a spiral can be seen at the bottom left of these snapshots, where black, white, and gray stripes are chasing each other.

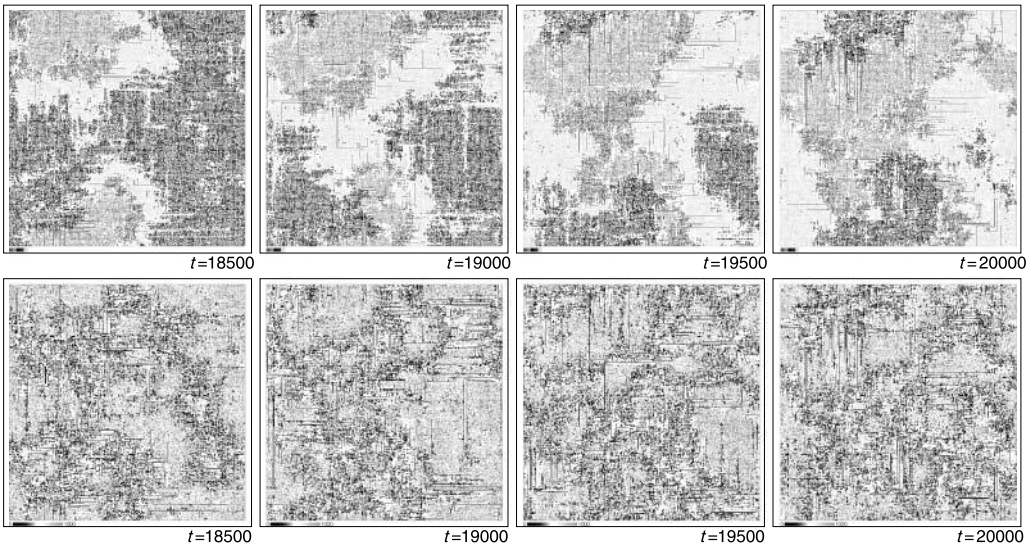

Figure 4. A spiral structure produced by five interacting species in a 400 × 400 cell space. The different species are illustrated with grayscales. The spiral rotates in a counterclockwise direction (upper series). The lifetimes of loops are shown as grayscale gradations in the lower series of snapshots, which represent the same run as the upper hand snapshots. In the lower series, light gray indicates loops that have lived more than 1000 time steps, whereas black indicates loops that are newly born. At the center of the spiral shown at the bottom left of the snapshots there are many new loops. Alternation of generations is faster in this region than in other regions (lower series).

The lower four images of Figure 4 show the lifetimes of loops as a grayscale gradation. Lighter gray represents older loops, whereas black represents younger loops. In the central region of the spiral at the bottom left of each snapshot, younger loops appear in greater numbers. New replicators are frequently born in these regions when a spiral structure is formed.

Populations of each species vary over time as they cycle around the center of the spiral. The periodicity of the variation is determined by the number of species in the food-web chain. Spirals consist of unstable oscillatory waves. In the case of less than four species, moving wavefronts are observed, but these fronts do not form complete spiral patterns. The reason appears to be that the length of the boundary between species is greater in this case, enabling loops from one species to more easily encroach on regions of an inferior species. This frequent encroachment prevents the formation of spiral patterns. Note that a similar result is found in more traditional spatially extended models of hypercycles, in which the minimum number of species for spiral formation is five. Occasionally, all loops of a species are destroyed, preventing the spiral structure from organizing, and leading eventually to dominance by a single species.

This type of spatiotemporal pattern, a spiral, is expected from former studies of, for example, spatially extended BZ reactions, prey-predator models, and hypercycles (see, e.g., [2]). It is thus not surprising that a food-web chain produces spiral or strip patterns. However, there are significant differences from those pattern formation studies. The spatiotemporal pattern in our case constitutes a source for intraspecific variation in new replicators. Differences between our model and a mere hypercycle system originate in the following characteristics of our loop replicators:

1. *Replication speed.* An offspring of a loop is not generated instantly. A finite number of time steps are required to replicate new generations. Within this period of offspring construction, an arm is extended from a parental loop to the position where the daughter loop will be created. Loop replicators are therefore fragile with respect to perturbations during this period. Such fragility has never been modeled in spatially extended hypercycles. Note also that there will be a natural selection of smaller loop replicators, as they breed more quickly.

2. *Internal degrees of freedom of replicators.* When S_i interacts with S_{i-1}, the latter loop is destroyed, but at the same time the invading loop S_i is modified in some complicated ways (described in Section 4). This naturally introduces *mutation* in the arm (gene) part of the replicator (S_i), so that variants will be generated during the interacting process.
3. *Long arm intrusion.* As a consequence of interspecies interaction, arms of loops may be extended abnormally far from the original parent structure. As can be seen in Figure 4, such species intrude tongue-like arms into the populations of neighboring species. These extended arms destabilize the spiral and strip structures.

As a consequence of these new features, variant replicating structures evolve depending on the spatiotemporal patterns. In particular, larger or non-square-shaped loops appear at the boundaries of spirals or strips. These larger loops can sometimes self-reproduce, and a colony of larger loop variants is generated. In the following two sections, we describe micro mechanisms of these variant replicating structures and analyze how they are controlled by the spatiotemporal patterns.

4 Mutational Dynamics

Various shapes and sizes of loops are deterministically generated by the interactions between individual loops. A variety of shapes and sizes arise from interaction-based mutations that cause irregular loop reproduction. Such irregular processes occasionally fail to replicate loops but sometimes generate new replication patterns.

In the following figures, we depict snapshots of irregular reproducing processes, taken from evolutions of minimal-sized loops in a five-species food-web chain replicating in the 400×400 cell space. The number of species in the food web may not be the significant parameter, at least if it is set larger than three.

4.1 Basic Mutation Processes

There are two major mutation patterns; (1) a point mutation in the gene entity and (2) intraspecific fusion of more than two loops. We report concrete examples of these and analyze the statistical significance.

4.1.1 Point Mutation of Genes

Self-replication of loops proceeds according to the gene sequence pattern coded in the `gene` fields of loops. Those genes are forwarded through the connecting cells that reproduce a new daughter loop at the tip of the arm. Without any perturbation, genetic information is transferred through a self-replication process forever. However, they may be lost during the replication process via interactions with other loops. In more detail, a gene loss occurs when the decoding process controlled by the DECODE mode cell at the tip of the arm is interrupted by the neighboring processes.

Figure 5 shows one example in which genes may be lost during the self-replication processes. This figure depicts the case in which interactions with inferior species cause a loss of genes. We also found that even the interaction between two loops of the same species often cause a loss of genes in similar ways (not shown here). By the gene loss processes, a daughter loop has a different shape from the parent loop. In the presented example, the daughter loop becomes smaller than the parent.

4.1.2 Intraspecific Fusion

Normal completion of the replication process occurs when the extended arm makes contact with its own structure. However, in general the arm may connect with itself or with the arm of a different loop of the same species. When two loops happen to collide with each other in specific ways, a novel shape may be created, as shown in the example of Figure 6. Because the new shape is encoded to

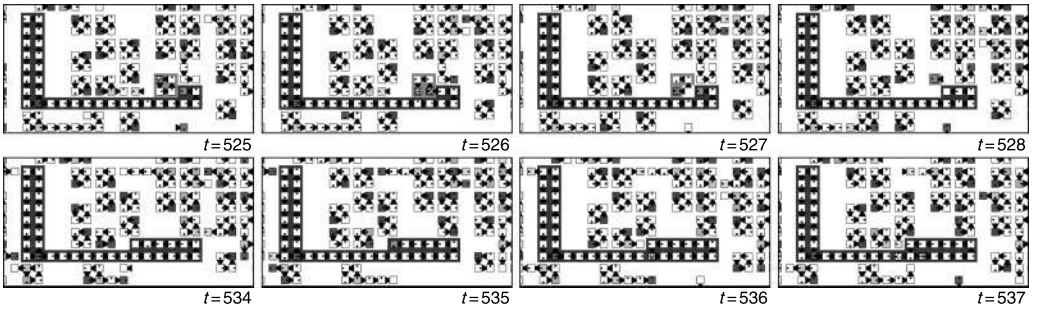

Figure 5. A smaller daughter loop is created by interaction-based mutation with a loop of an inferior species. A loop of species S_i (dark gray) collides with another loop of an inferior species S_{i-1} (light gray) via the inroad interaction. In this process, the tip of the S_i loop is not able to decode certain genes, because there exist cells of the S_{i-1} loop in the target site (t=525, t=526). Because of the loss of the two C genes, the daughter loop that is constructed becomes smaller than the original parent loop (t=536).

genes via the normal encoding mechanism, the emergent loop is also capable of replicating itself, as well as the parent loop. Sometimes, emergent loops have irregular internal states, for example, containing multiple ENCODE-mode cells or multiple BRANCH-mode cells. This abnormal situation causes irregular replication and reduces the accuracy of self-replication.

To investigate the statistical nature of such processes in our system, we classified the mutation processes into four types: (1) normal self-replication events, (2) mutation events involving no other loops than the parent (point mutation), (3) intraspecific fusion with other loops, and (4) other types of mutation events (Figure 7).

Frequencies are counted over 10,000 time steps and averaged over 10 different runs. In the case of the smallest (four-cell) loop, a normal replication is the dominant event. Both mutations and normal replication frequencies tend to increase on increasing the loop size. In fact, the frequency of the normal replication events roughly obeys a power law. Loops of a size larger than 30 are created exclusively via fusion. Finally, one example of the fourth type of mutation event [type (4) above] occurs when the fragments of partially dissolved loops are arranged into a loop shape accidentally. If this loop has appropriate modes (e.g., one BRANCH mode), it can self-replicate. This particular event is only observed in the smallest four-cell loops.

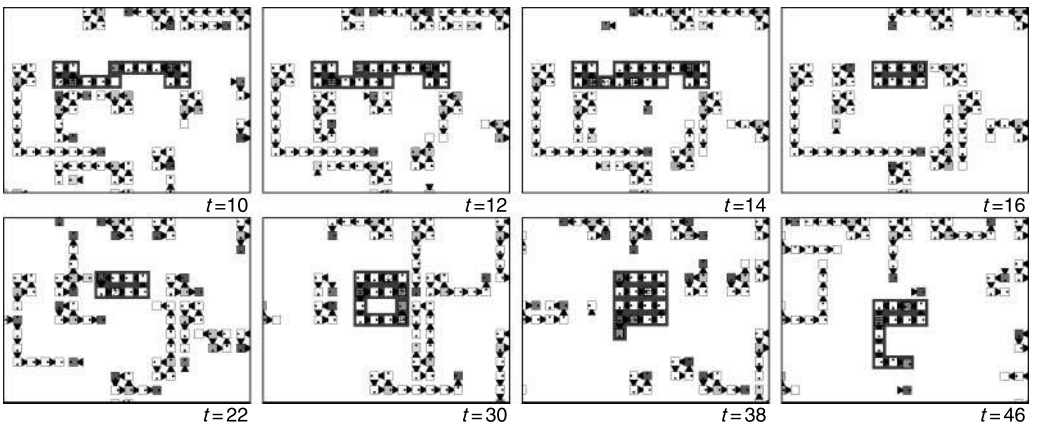

Figure 6. When two loop arms connect as they are each making the first left turn in the arm extension phase of the self-replication process, the arms become merged together, often leading to the emergence of a new loop. This type of event was frequently observed in our simulations and was found to lead to an increase in the overall variation of loop shapes within a population.

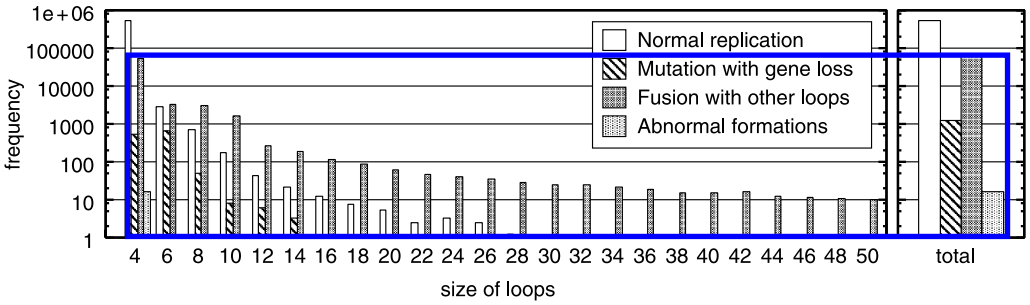

Figure 7. The frequency of four different types of replication events (log scale): (1) normal self-replication events, (2) mutation events originated by gene losses, (3) mutation events by fusion of other loops, and (4) other atypical mutation events. The left-hand graph shows the frequency of loops for different loop sizes, and the right-hand graph shows the total frequency summed over all loop sizes. Initially, four-cell loops are randomly distributed in the 400×400 space. Frequencies are summed over 10,000 time steps and are averaged over ten different runs.

4.2 Open Extended Arm Structures and Irregular Self-replication

The irregular behaviors of loops provide functional changes to loop replication.

One example is that gene loss in point mutation causes the loop arms to extend abnormally. This situation occurs if the L gene is lost that is responsible for a left turn in the extended arm. If this gene is lost, the extended arm continues to create new cells in the forward direction rather than closing and completing the replication process (Figure 8). Such open extended arms act as a part of the environment, and make the global spiral pattern unstable (as mentioned earlier in Section 3).

Open extended arms can also provide another source of irregular behavior. Figure 9 shows two loops fusing to produce one daughter loop. In cases such as this one, the shape of the daughter loop is the same as that of the parent. However, because fusion occurs with the operation arm extended abnormally far from the parent, the arm becomes a conduit through which genes can travel a long distance across the CA domain. It enables loops of a superior species to advance deeply and rapidly into the territory of an inferior species, extending the region of S_1 into the adjacent region of S_2.

In order to investigate the above-mentioned irregular self-replicating process, we further classified fusion-based mutation into four categories with respect to size changes: (1) no size change (irregular replication), (2) smaller size change, (3) larger size change, and (4) unidentified size change (Figure 10). Because the operation arm may merge several times during the fusion process, the parent loop is often difficult to identify. We here define a parent loop as the loop connected to the operation arm when construction of the daughter loop is completed. Still, in some cases, it is difficult

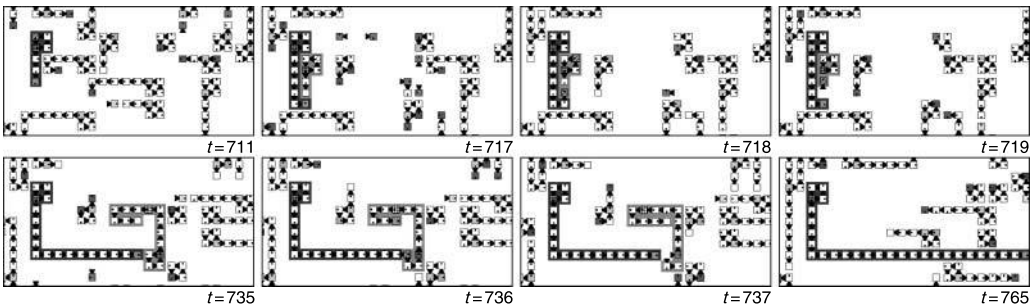

Figure 8. Collision with a loop of an inferior species (light gray) triggers indefinite extension of the operation arm of the superior species (dark gray). The arm continues to extend until it contacts the loop of a superior species or one of the same species.

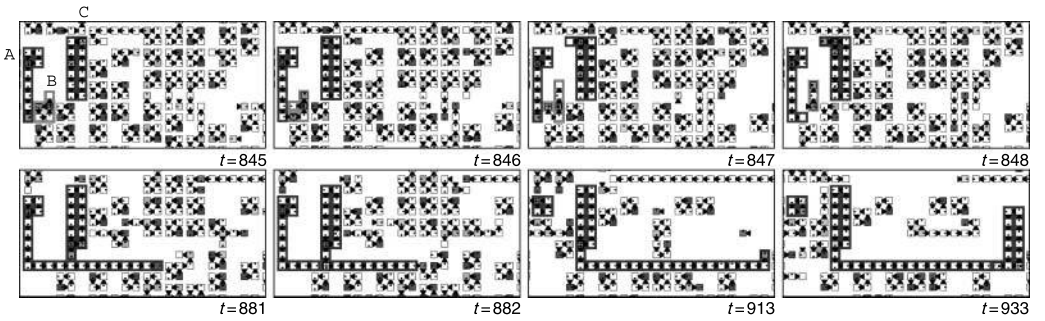

Figure 9. An example of fusion between two colliding loop structures. A four-cell loop (marked A) collides with a loop of an inferior species (marked B). The result is that two L genes in loop A are not decoded (t=845, t=846), and thus the loop, rather than constructing a square-shaped offspring as it otherwise would, instead extends its operation arm indefinitely. A twelve-cell loop on the right, of the same species as loop A (marked C), collides with loop A and interrupts this indefinite arm extension, fusing the two arms together. With arms fused together, genes of loop C are redirected through the arm structure constructed by loop A. Loop C utilizes this extended arm structure to replicate itself, causing the daughter loop to be constructed a great distance away from the parent.

to identify a parent loop. Such an example can be found in Figure 6. When a large loop fuses with other loops, the resulting loops tend to get larger. In particular, almost all loops of size greater than about 20 increase their size after the fusion process. However, small loops not only change their size, but also replicate themselves, even through fusion. This indicates that the fusion process results not only in change of size, but also in gene transportation, as illustrated in Figure 9.

Mutation events such as the ones described so far generate a variety of variant replicating structures. Interactions between loops cause the loss of some genes, leading to the generation of different shapes of loops. In particular, the fusion of multiple loops into a single daughter generates a number of larger loops. It is worth noting that the mutation may affect not only the shape of the loop, but also the replication process itself. The long extending arm, formed by loss of genes, can be used as a path for information on the shape of a parent loop. As a result, a daughter loop can be generated at a distance (Figure 9). When the place where the daughter loop is created is suitable for replication, such as a region of inferior species, the loop can survive longer than when the daughter loop is created near the parent. Thus, how the loop replicates itself in an advantageous space may be an important criterion for survival.

With interaction-based mutation, loops have the potential to produce a variety of larger replicators. However, that such larger loops can survive for extended periods of time in competition with other loops has not yet been established. In the next section, we will demonstrate the survivability and robustness of these larger variant loops.

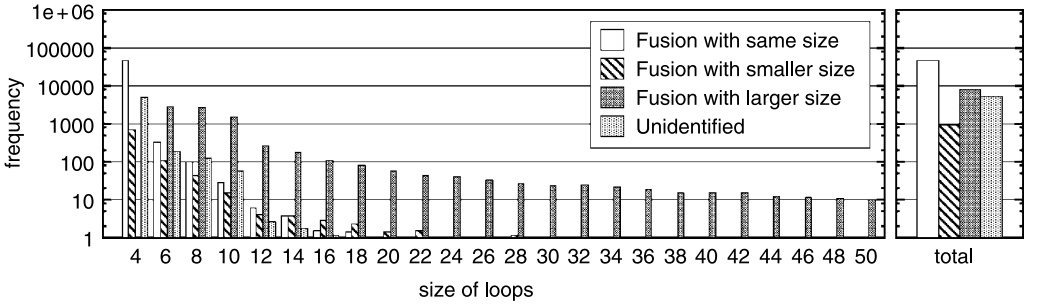

Figure 10. The frequency of mutation events involving fusion of other loops, categorized with respect to change in the loop size. The left-hand graph shows the frequency of loops of different sizes, and the right-hand graph shows the total frequency summed over all loop sizes. Initially, four-cell loops are randomly distributed in the 400×400 space. Frequencies are summed over 10,000 time steps and are averaged over ten different runs.

5 A Mechanism for Synthesizing Larger Loops

The mutational dynamics discussed so far does not directly lead to the emergence and reproduction of larger loops. Large loops are disadvantaged in that they require more time steps than smaller loops to carry out self-replication. Therefore larger loops generally disappear soon after they appear. The CA space will finally be dominated by the smallest, size-4 loops. We have observed that the larger loops do, however, sometimes manage to replicate themselves at the boundary between different species.

In this section, we report successful replication of larger loops on the boundary, and quantify the process. Further, the population dynamics of the large loops is investigated. In the following subsection, we construct genealogy trees of loop replicators to study their lifetimes and diversification. A system with an initial random distribution of four-cell loops is simulated on the 400×400 cell space.

5.1 Emergence of Larger Loops at the Boundary between Species

A main reason for the generation of large loops at a boundary is that the boundary is the interface between superior and inferior species in the spiral hypercycle formation. While intraspecific collisions occur within a region, as we see in Figure 11, at the boundary between regions, large loops form colonies and outperform the minimal-loop population.

First, at the boundary between species, superior loops frequently collide with inferior loops by using the inroad interaction. Mutations of genes leading to variant loops occur much more frequently by this type than by the other types of interaction classified in Section 2.3. Second, the region of inferior species along the boundary provides a vacant space for the superior species, where their larger loops will be bred. Moreover, as shown in Section 4.2, fusion often creates abnormally long arms that fail to close to form daughter loops, instead extending indefinitely into the region of inferior species. These extended arms occasionally generate variant daughter loops in the middle of the population of inferior loops (Figure 11). When this happens, such larger loops rapidly increase their numbers. Creation of these variant loops perturbs the spiral structure and makes it unstable. This never occurs in hypercycle models of replicators with no internal structural dynamics [2].

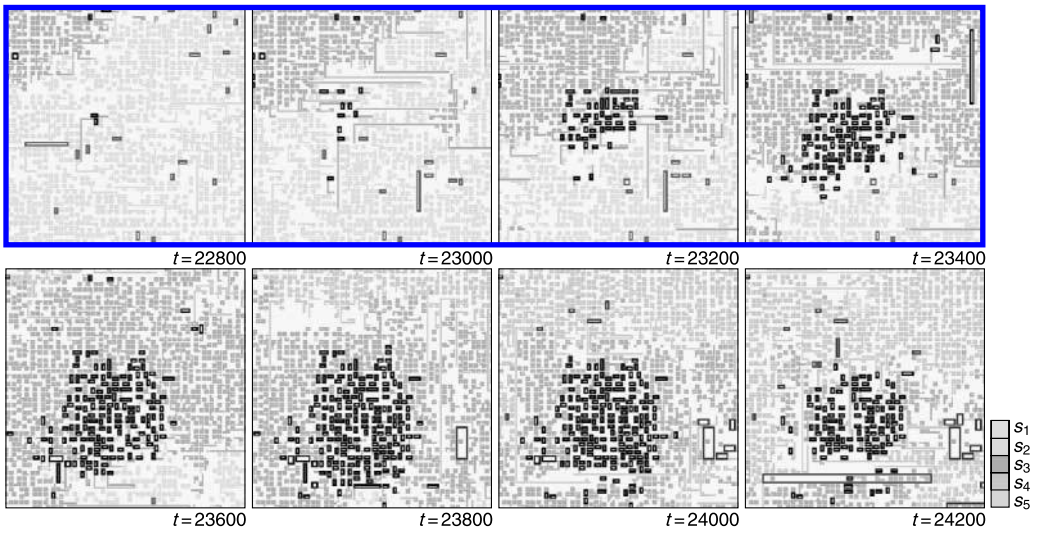

Figure 11. An example of the emergence of larger loops inside the population of inferior loops at the boundary between species. The loops of size greater than 6 are highlighted in darker shades. A colony of mainly size-6 loops appears and grows as loops of the superior (S_3) species invade the population of loops of the inferior (S_2) species. However, the larger loops are destroyed by the invasion of S_4 species (superior to S_3) and cannot survive for a long period of time. Subsequently, larger loops from the S_4 species emerge and grow in this region.

To quantify how the larger loops replicate and interact with each other, we introduce a new quantifier, which measures the spatial density of the neighboring loop sizes. By using the loop size i and the distance r_{ij} between two loops, we calculate the measure as follows:

$$B = \frac{1}{2N^2} \sum_i \sum_{j<i} \frac{l_i l_j}{b_{ij}^2 r_{ij}^2}, \quad b_{ij} = \begin{cases} l_i - l_j & \text{for} \quad l_i \neq l_j \\ 0.1 & \text{for} \quad l_i = l_j \end{cases}$$

The variable b_{ij} was introduced to reflect the difference of neighboring loop sizes. For the analysis of the larger loops, we only considered the loops whose sizes are greater than 4 in the above summation. The measure B becomes large when the same large loops aggregate at one point.

We calculate the value of this quantifier for five different experiments. The first four experiments involve single-species populations in which one of the four interaction rules described in Section 2.3 is used exclusively; this allows us to investigate each rule in isolation from the other rules. The fifth experiment includes all four rules of the food web with five species. Figure 12 shows the difference between single-species and competitive systems. In the case of the cancel, counter, and inroad rules, larger loops cannot become abundant. Due to the definition of the measure B, the values of the

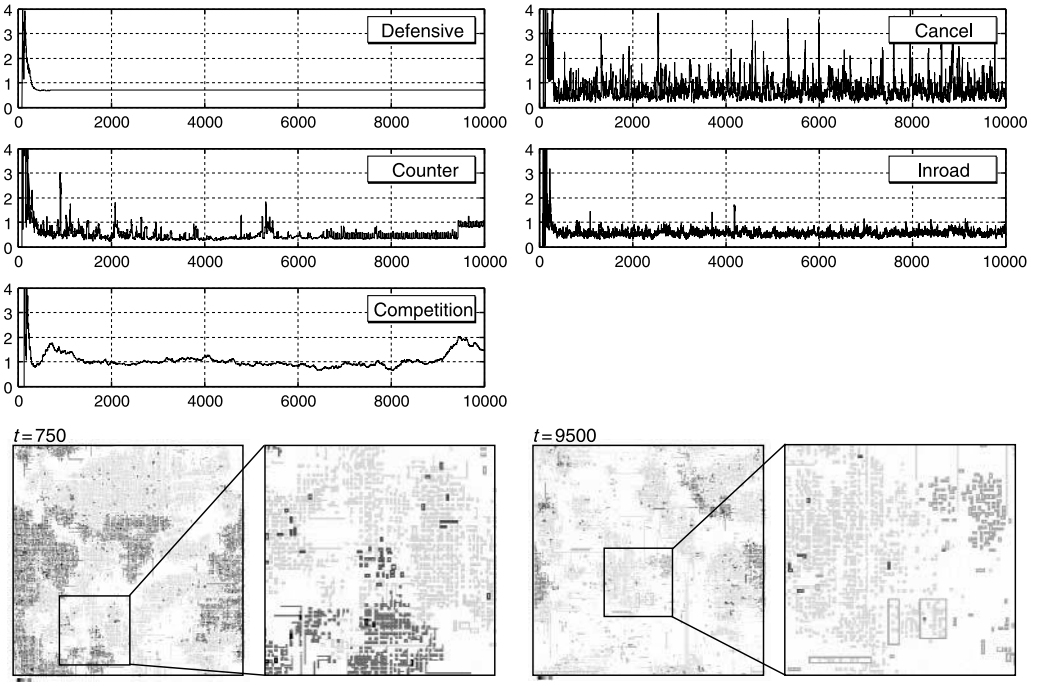

Figure 12. In the upper graphs, the quantifier is calculated for each of the four experiments with single-species populations ("defensive," "counter," "cancel," and "inroad") as well as for the experiment with five species and all interaction rules ("competition"). The value represents how often large loops emerge locally. Experiments were initiated with four-cell loops randomly distributed in a 400×400 cell space. In each case, the CA space is initialized with an ancestor population of size-4 loops at a density of 0.05%. In the five-species case, populations of all five different species are equally distributed at the start of the run. In the case of the cancel rule, because the number of large loops is low ($10-10^2$), the value of B fluctuates significantly. Compared with the other experiments, B has high values at all times for the competition. In the lower part of the figure, screenshots depicting the emergence of large loops for the five-species experiment are shown at t=750 and t=9500. These peaks in the upper graph for the competition experiment reflect the clustering of larger loops depicted in the snapshots. The loops of size greater than 6 are highlighted with darker shades.

quantifier fluctuate in the case of the cancel rule; this is because this rule sustains only a small amount of population. The relative number of larger loops in the population can increase under the defensive and competition rules. Comparing the fifth with the four single-species experiments, we notice that the quantifier maintains a high value under the competition rule. The bottom images of Figure 12 show screenshots taken when the quantifier shows the maximal value. The local increase of the number of larger loops is responsible for this increase.

Figure 13 shows that both population size and boundary length oscillate globally, where the boundary length between two species is defined as the number of cells of one species that are directly adjacent to cells of the other species. Other species show the same oscillatory behavior but with different phases. The associated spatial pattern is a spiral in which species S_{i+1} is followed clockwise by species S_i. The larger loops emerge at the boundaries between species and start to reproduce as shown in Figure 11. The frequency of emergence of larger loops increases when the boundary length increases, as can be seen in Figure 13 (bottom). We thus conclude that the boundaries between species contribute to periodic emergence of larger variant loops.

5.2 Genealogy Tree and Size Distribution

The genealogy of a single species of different interaction types (as in Figure 14) is compared with those of competing cases. In the single-species models, only one of the interaction rules (defensive, counter, cancel, and inroad) is used as a rule for the interloop interaction.

The first four parts of Figure 14 show examples of genealogy trees for the four single-species models (each corresponding to a different interaction rule); the last part depicts the five-species case with the full set of cyclic interaction rules. The same set of parameters of the simulation is used in this case. The initial population is composed exclusively of four-cell loops.

Branching (corresponding to variant loops) is observed as splitting from the original root tree. With the defensive interaction, each branch is robust and new branches extend for long periods of time. Larger branches, however, are created rather infrequently. In contrast, lifetimes of branches are very short with the cancel interaction. Branches with larger size are often generated, but they vanish

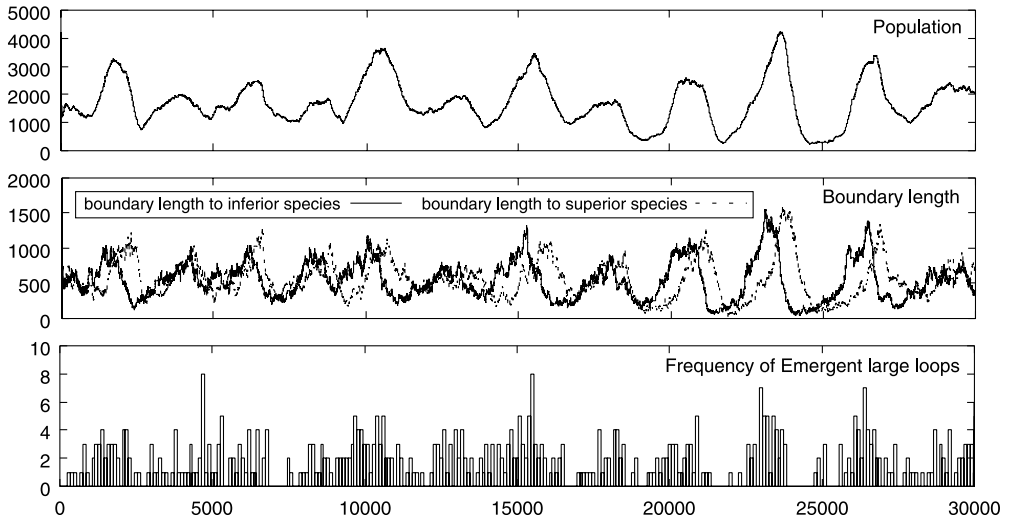

Figure 13. Population dynamics, boundary length, and frequency of emergence of large loops for one of the five species in a food web. Temporal variation of the loop population (top) seem to be accompanied by changes in the boundary length (middle). The number of large loops (size $\geq$ 20) increases whenever the length of the boundary from superior to inferior species increases (bottom). The system size is 400×400 cells. The population is initiated with four-cell loops from a five-species food web.

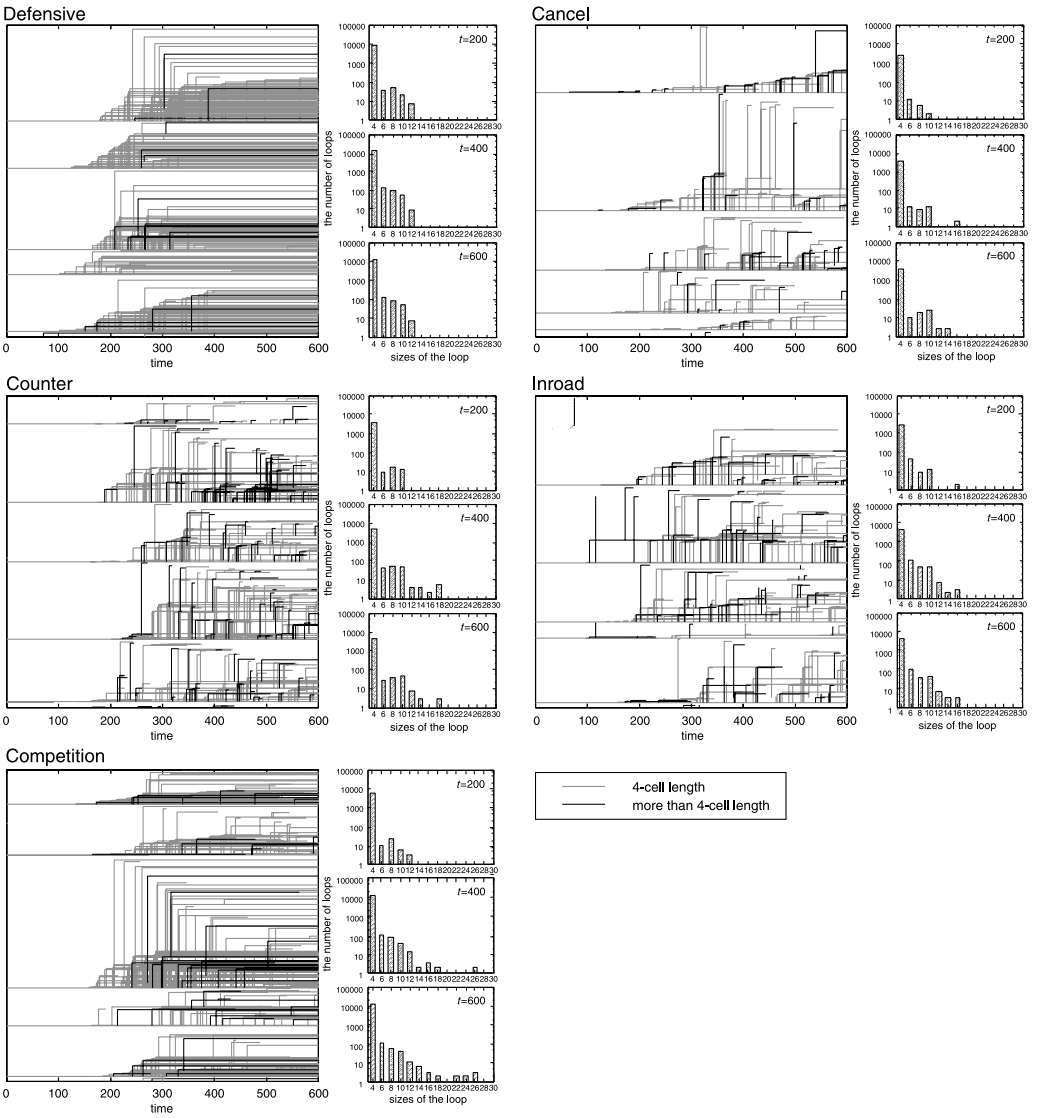

Figure 14. Part of the genealogy tree for the four single-species populations (defensive, counter, cancel, and inroad) as well as the five-species food web (up to time step 600). Four-cell loops are initially randomly distributed in a 400×400 cell space. Each branch corresponds to the detecting of a newly constructed daughter loop from a parent loop. A new branch is created when a loop is constructed either by two parent loops or by other types of accidental collision events. Each horizontal branch indicates how long the corresponding loop survives. The vertical lines show when and from which branch (of a parent loop) a new loop split off. The loops of average size greater than 6 are highlighted in darker shades. Loop size distributions at time steps 200, 400, and 600 are also associated with each main graph. The accumulated data is given in Figure 15. Note that the four single-species experiments correspond to homogeneous single-species populations operating according to one of the four specific interaction rules (not the full set of cyclic interactions). For details, see the text.

soon as well. The counter and inroad interactions can generate larger branches that persist for some time. However, their lifetimes are still shorter than those of 4-cell-length loops, so that the branches vanish before they show further branching. The defensive interaction does not destroy loops when the interaction occurs. In contrast, with the cancel, counter, and inroad interactions, loops are easily destroyed by the interactions, but also generate variant loops.

Finally, the competitive food-web chain retains features of both the defensive and inroad cases. It has a large number of long-lasting branches and an increased number of larger replicators. Spatial coexistence of multiple interactions that have different strengths of protection is one reason for the distinctive properties of the competitive food-web system.

Figure 15 shows a computed size distribution of replicating loops corresponding to Figure 14. The results are accumulated over 10,000 time steps. As is clearly seen from the figure, the food-web model produces the largest number of loops of size greater than 30 cells. As we discussed in the previous section, the formation of vacant space is responsible for developing larger loops.

6 Discussion

Although the model we have presented in this article is completely determined by a fixed set of CA rules, we can draw some general conclusions based on observations of its behavior. In particular, we can understand its evolutionary dynamics in terms of the relationships between micro and macro levels, macro being the spatial scale of (e.g.) spiral formation, and micro being the scale of the individual replicator.

In Section 3, we showed the effect of spatial patterning on the evolution of self-replicating loops. We can easily have strips and spirals in those multispecies reactive media. In particular, spiral formation has been shown to be evolutionarily advantageous in that it leads to resistance against parasites [2]. Also, Hamilton stressed the importance of spatial patterning in evolutionary systems [5]. In our model, global spiral patterns continuously provide effectively vacant space (regions occupied by inferior species) for loops to self-replicate. As shown in Section 5, by utilizing this space, self-replicators are able to mutate toward larger size, and more complex structures can emerge. We argue that the evolvability and survivability of self-replicating loops are affected by this macro spatial patterning. This is an interesting example of how macro-scale phenomena affect the underlying micro phenomena.

From a microscopic and local-rule point of view, the source of the micro-macro relationship is resolved into the way a loop interacts with other loops. Recently, Sayama independently studied the relationship between a similar set of interaction rules and the diversity of new emergent loops [19]. Using these rules, he investigated aspects of self-protection and robustness in his system of self-replicating loops. The rules he used for realizing self-protection correspond roughly to the defensive interaction rule in our model. A difference in his model, however, is that loops cannot protect themselves against collisions that involve any of the corners of the rectangular form of a loop. He insisted that this weakness of the self-protection mechanism in his model enables the evolutionary process to generate a diversity of different loop shapes. In our system, in contrast, the defensive rule enables complete protection; there are no hidden vulnerabilities such as corners. This rule alone, however, cannot produce much diversity in the shapes of emergent loops. The other types of

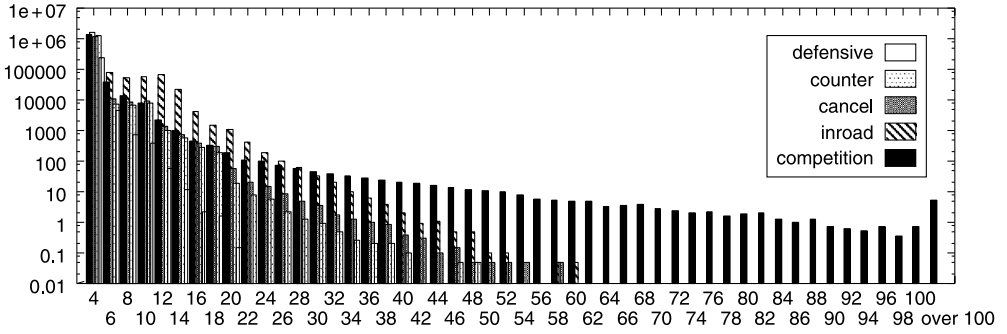

Figure 15. Frequency histogram of loop sizes. A vertical bar represents the total number of loops of a particular size observed during 10,000 steps. The initial state only includes loops of size 4. The CA space has 400×400 cell sites. Loops larger than size ≈50 only emerge in the competition model.

interaction (cancel, counter, and inroad rules) play a critical role in the emergence of such diversity. It is by including all interaction types that we expect to arrive at the development of a diverse set of robust self-replicators, possibly including larger, more complex ones.

Many of the complex loops that emerge in our simulations originate in some kind of fusion process. Fusion of neighboring loop structures is possible because, while undergoing self-replication, loop structures cannot distinguish their own body from that of another replicator. This ambiguous boundary between organism and organism enables a diversity of different loop shapes to arise. In Ray's Tierra system, some programs can replicate by utilizing the replication machinery of other programs. Such programs are called "cheaters" or parasites. In our model, the fusion of loops constitutes a similar phenomenon. Loops that extend their arms into collisions with the arms of other loops can contribute gene sequences toward construction of the daughter loop. This results in the emergence of daughter loops at locations in space very distant from the parent loop (Section 4.2). This phenomenon can be seen as a similar "cheating" replication by utilizing the other organism's spatial structure.

To conclude, we note that while in the present model the microscopic dynamics of replication are affected by the macroscopic dynamics (of, e.g., spiral formation), there is no corresponding effect of macroscopic patterns on microscopic dynamics. Indeed, a diverse range of micro-scale replicator dynamics gives rise to similar macro-scale patterns. However, we suspect that a model *with* such a circular relationship between the macro- and micro-scale dynamics may indeed display open-ended evolution.

Acknowledgments

We thank Duraid Madina for critical reading of the manuscript. This work was partially supported by grants-in-aid from the 21st Century COE (Center of Excellence) program (Research Center for Integrated Science) of the Ministry of Education, Culture, Sports, Science, and Technology, Japan.

References

1. Bedau, M., McCaskill, J., Packard, N., Rasmussen, S., Adami, C., Green, D., Ikegami, T., Kaneko, K., & Ray, T. (2000). Open problems in artificial life. *Artificial Life*, *6*(4), 363–376.
2. Boerlijst, M. C., & Hogeweg, P. (1991). Spiral wave structure in pre-biotic evolution: Hypercycles stable against parasites. *Physica D*, *48*, 17–28.
3. Chou, H., & Reggia, J. (1997). Emergence of self-replicating structures in a cellular automata space. *Physica D*, *110*, 252–272.
4. Dewdney, A. K. (1988). *The armchair universe: An exploration of computer worlds*. New York: W. H. Freeman.
5. Hamilton, W. D. (1999). Fables of cyberspace: Tapeworms, horses, and mountains. *Proceedings of the Fifth European Conference on Advances in Artificial Life* (pp. 5–6). Berlin: Springer-Verlag.
6. Ibáñez, J., Anabitarte, D., Azpeitia, I., Barrera, O., Barrutieta, A., Blanco, H., & Echarte, F. (1995). Self-inspection based reproduction in cellular automata. *Proceedings of the Third European Conference on Advances in Artificial Life* (pp. 564–576). Berlin: Springer-Verlag.
7. Ikegami, T. (1994). From genetic evolution to emergence of game strategies. *Physica D*, *75*, 310–327.
8. Libson, H., & Pollack, J. B. (2000). Automatic design and manufacture of robotic lifeforms. *Nature*, *406*, 974–978.
9. Langton, C. G. (1984). Self-reproduction in cellular automata. *Physica D*, *10*, 135–144.
10. Lindgren, K. (1992). Evolutionary phenomena in simple dynamics. *Artificial Life II: Proceedings of the Workshop on Artificial Life* (pp. 295–312). Redwood City, CA: Addison-Wesley.
11. Morita, K., & Imai, K. (1997). A simple self-reproducing cellular automaton with shape-encoding mechanism. *Artificial Life V: Proceedings of the Fifth International Workshop on the Synthesis and Simulation of Living Systems* (pp. 489–496). Cambridge, MA: MIT Press.
12. Ray, T. S. (1992). An approach to synthesis of life. *Artificial Life II: Proceedings of the Workshop on Artificial Life* (pp. 371–408). Redwood City, CA: Addison-Wesley.

13. Salzberg, C., & Sayama, H. (2004). Complex genetic evolution of artificial self-replicators in cellular automata. *Complexity*, *10*(2), 33–39.

14. Salzberg, C., Antony, A., & Sayama, H. (2004). Evolutionary dynamics of cellular automata-based self-replicators in hostile environments. *BioSystems*, *78*, 119–134.

15. Sayama, H. (1998). Introduction of structural dissolution into Langton's self-reproducing loop. *Artificial Life VI: Proceedings of the Sixth International Conference on Artificial Life* (pp. 114–122). Cambridge, MA: MIT Press.

16. Sayama, H. (1999). A structurally dissolvable self-reproducing loop implemented from Langton's self-reproducing loop (in Japanese). *IPSJ Transactions SIG2(TOM1)*, *40*, 55–67.

17. Sayama, H. (1999). A new structurally dissolvable self-reproducing loop evolving in a simple cellular automata space. *Artificial Life*, *5*(4), 343–365.

18. Sayama, H. (2000). Self-replicating worms that increase structural complexity through gene transmission. *Artificial Life VII: Proceedings of the Seventh International Conference on Artificial Life* (pp. 21–30). Cambridge, MA: MIT Press.

19. Sayama, H. (2003). Self-protection and diversity in self-replicating cellular automata. *Artificial Life*, *10*(1), 83–98.

20. Sims, K. (1994). Evolving virtual creatures. *Proceedings of SIGGRAPH 94* (pp. 15–34). New York: ACM Press.

21. Tempesti, G. (1995). A new self-reproducing cellular automaton capable of construction and computation. *Proceedings of the Third European Conference on Advances in Artificial Life* (pp. 555–563). Berlin: Springer-Verlag.

22. von Neumann, J. (1966). *Theory of self-reproducing automata*. Urbana, IL: University of Illinois Press.

Appendix 1: State Transition Rules for the Single Loop

A1.1 Labeling of the Cell Neighborhood

As illustrated in Figure 16, each cell has four neighbors. We refer to the cell pointed to by the `link` field of the center cell as the *rear neighbor*. All other neighbors are together referred to as the *front neighbors*. The neighboring cell whose gene points to the center cell is called the *neighbor with gene directed toward the center cell*. The center cell is always either in the `quiescent` state or in one of the structure states. The structure state is further classified into four different fields. Depending on the value of each field in neighboring cells, a cell may behave in different ways, as described below.

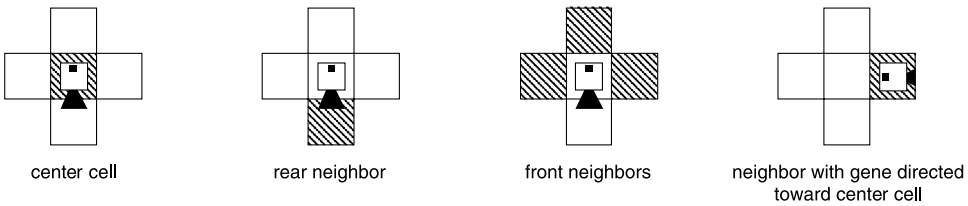

Figure 16.

A1.2 `quiescent` State

A1.2.1 Transition from `quiescent` State

In Figure 17:

(a) If one cell in the neighborhood is in DECODE mode, and this cell has a gene directed toward the center cell, then the center cell becomes a `structure` state with no genes in the NORMAL

mode. The `link` field of the center cell is directed toward the neighboring cell from which the gene was propagated.

(b) If two or more cells in the neighborhood are in DECODE mode, and these cells have a gene directed toward the center cell, then the center cell remains in the `quiescent` state.

(c) In all other cases, the center cell remains in the `quiescent` state.

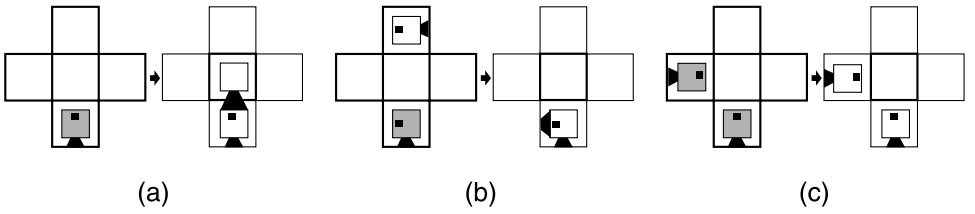

Figure 17.

A1.3 `structure` State

A1.3.1 For All the `structure` States

In Figure 18:

(a) Any structure cell with no structure cell as its rear neighbor immediately switches to the `quiescent` state.

(b) Otherwise, if any neighbor is in DESTROY mode with its gene directed toward the center cell, then the `gene` field of the center cell is redirected to line up with its (previous) `link` field, after which its `link` field is updated to point to the location of the DESTROY-mode cell. The mode of the center cell is switched to DESTROY mode.

(c) In all other cases, if the center cell is not in BRANCH mode, and a cell in WITHDRAW mode with a gene directed toward the center cell exists in the neighborhood, then the `gene` field of the center cell is redirected to line up with its (previous) `link` field, after which its `link` field is updated to point to the location of the DESTROY-mode cell. The mode of the center cell is switched to WITHDRAW.

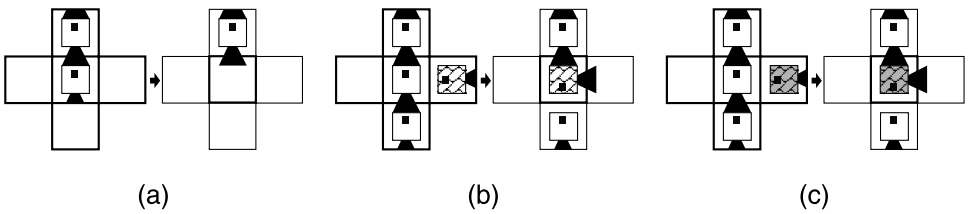

Figure 18.

A1.3.2 For the NORMAL Mode

In Figure 19:

(a) If any of the front neighbors are in DECODE mode with a gene directed toward the center cell, then the `link` field of the center cell is redirected to point to this DECODE-mode cell. The `gene` field of the DECODE-mode cell is copied to the center cell, and the center cell switches to BRANCH mode.

(b) Otherwise, if the rear neighbor is in ENCODE II mode, then the center cell switches to ENCODE I mode. The `gene` field of the ENCODE II-mode cell is copied to the center cell.

(c) Otherwise, if the rear neighbor is in EXPLORE mode:

(i) If the center cell is connected to another front left neighbor cell, and the neighboring cell in the direction of the `gene` field of the EXPLORE-mode cell is empty, then the center cell switches to DECODE mode. The `gene` field of the EXPLORE-mode cell is copied to the center cell.

(ii) In all other cases, the center cell switches to EXPLORE mode. The `gene` field of the EXPLORE-mode cell is copied to the center cell.

(d) Otherwise, if there is no neighboring `structure` cell for which the center cell is a rear neighbor:

(i) If one of the front neighbors is in EXPLORE mode, then the `link` field of the center cell is redirected to point to the position of the EXPLORE-mode cell, and the center cell switches to WITHDRAW mode. The `gene` field of the center cell is directed to point in the same direction as its `link` field.

(ii) In all other cases, the `gene` field of the rear neighbor is copied to the center cell, and the center cell mode switches to DECODE.

(e) Otherwise, if there is a cell in BRANCH mode for which the center cell is a front left neighbor, then the `gene` field of the center cell is reset to the C state. The center cell remains in NORMAL mode.

(f) In all other cases, the `gene` field of the rear cell is copied to the `gene` field of the center cell. The center cell remains in NORMAL mode.

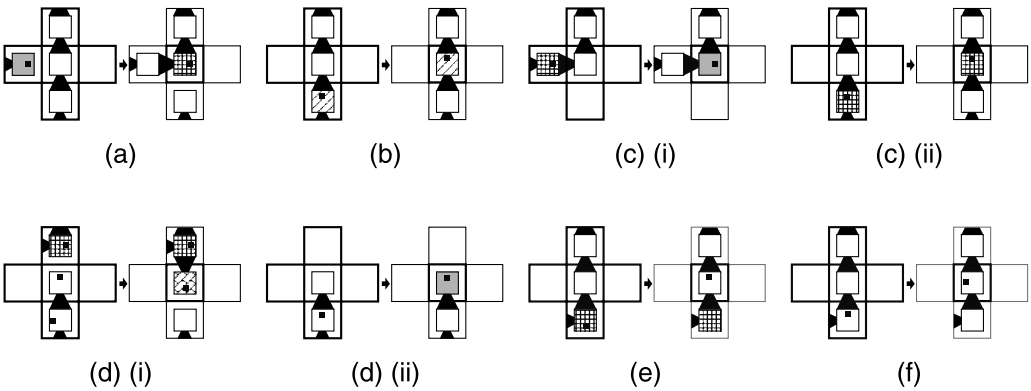

Figure 19.

A1.3.3 For the DECODE Mode

In Figure 20:

(a) If there is no neighboring `structure` cell for which the center cell is a rear neighbor, then the center cell switches to NORMAL mode. The `gene` field of the rear cell is copied to the `gene` field of the center cell.

(b) Otherwise, if the `structure` cell whose rear neighbor is the center cell is a left front neighbor of the center cell, then the center cell switches to BRANCH mode. The `gene` field of the rear cell is copied to the `gene` field of the center cell.

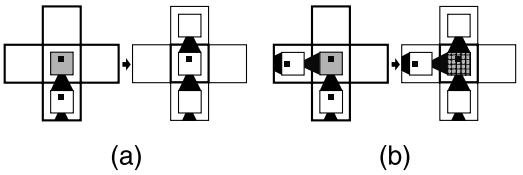

Figure 20.

A1.3.4 For the ENCODE I Mode

In Figure 21:

(a) If the rear neighbor is in EXPLORE mode, the center cell switches to EXPLORE mode. The `gene` field of the rear neighbor is copied to the `gene` field of the center cell.

(b) Otherwise, if one of the front neighbors is a `structure` cell, and the rear neighbor of this `structure` cell is the center cell, then the `gene` field of the center cell is redirected to point to the location of the `structure` cell. The center cell switches to ENCODE II mode.

(c) In all other cases, the `gene` field of the center cell is reset to C. The center cell switches to ENCODE II mode.

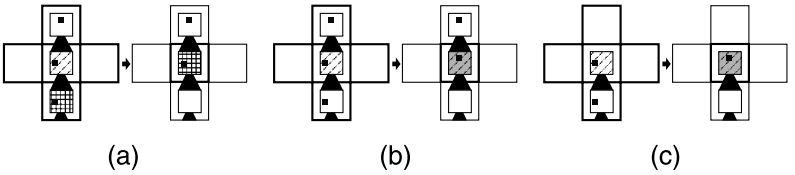

Figure 21.

A1.3.5 For the ENCODE II Mode

In Figure 22:

(a) If the rear neighbor is in ENCODE II mode, then the center cell remains in ENCODE II mode. The `gene` field of the rear neighbor is copied to the `gene` field of the center cell.

(b) Otherwise, if the rear neighbor is in EXPLORE mode, then the center cell switches to EXPLORE mode. The `gene` field of the rear neighbor is copied to the `gene` field of the center cell.

(c) In all other cases, the center cell switches to NORMAL mode. The `gene` field of the rear neighbor is copied to the `gene` field of the center cell.

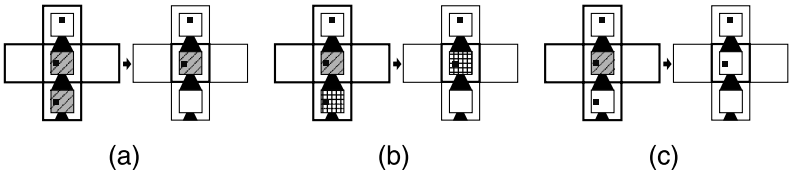

Figure 22.

A1.3.6 For the BRANCH Mode

In Figure 23:

(a) If any of the front neighbors are in WITHDRAW mode with a gene directed toward the center cell, the center cell switches from BRANCH mode to EXPLORE mode. The `gene` field of the rear neighbor is copied to the `gene` field of the center cell.

(b) In all other cases, the center cell remains in BRANCH mode. The `gene` field of the rear neighbor is copied to the `gene` field of the center cell.

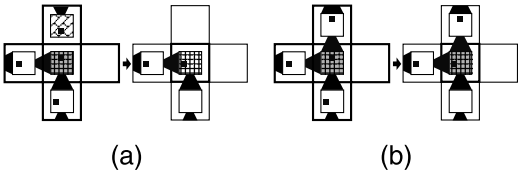

Figure 23.

A1.3.7 For the EXPLORE Mode

In Figure 24, the center cell switches from EXPLORE mode to NORMAL mode. The `gene` field of the rear neighbor is copied to the `gene` field of the center cell.

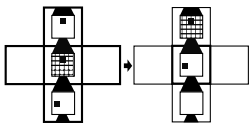

Figure 24.

A1.3.8 For the WITHDRAW Mode

In Figure 25, the center cell switches from WITHDRAW mode to the `quiescent` state.

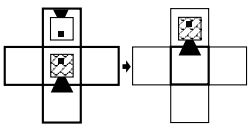

Figure 25.

A1.3.9 For the DESTROY Mode

In Figure 26, The center cell switches from DESTROY mode to the `quiescent` state.

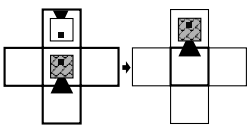

Figure 26.

Appendix 2: State Transition Rules for Interactions between Loops

A2.1 Transmission of `species` Field Labels

The `species` field is only changed in the situation in which the center cell is in the `quiescent` state and just one neighbor is in DECODE mode with its `gene` field directed toward the center cell. In this

case, the `species` field is copied from the neighboring `structure` cell into the center cell. All other transitions are the same as those for the single loop described above. Note that the transition rules for a single loop as shown in Figures 17–26 are only applied between cells that have the same species label. Between cells with different species labels, the interaction rules shown in Figures 27 and 28 are applied.

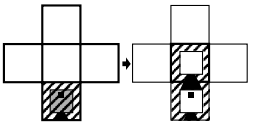

Figure 27.

A2.2 Interaction Rule for DECODE Mode

If the front neighbor pointed to by the `gene` field of the center cell is a `structure` cell, then depending on the interaction type, one of the following transition rules (Figure 28) is applied:

(a) Defensive (non-left-side): If the center cell is the front left neighbor of the `structure` cell, then the `gene` field is redirected to line up with its (previous) `link` field, after which its `link` field is updated to point to the location of the `structure` cell. The center cell then switches to WITHDRAW mode.

(b) Defensive (left-side): In other cases, the transition rule for the single loop is applied.

(c) Counter, (d) cancel: The `gene` field from the rear neighbor is copied to the center cell. The center cell's `link` field is redirected to point to the `structure` cell. The center cell switches to DESTROY mode.

(d) Inroad: The `gene` field of the rear cell is copied to the `gene` field of the center cell.

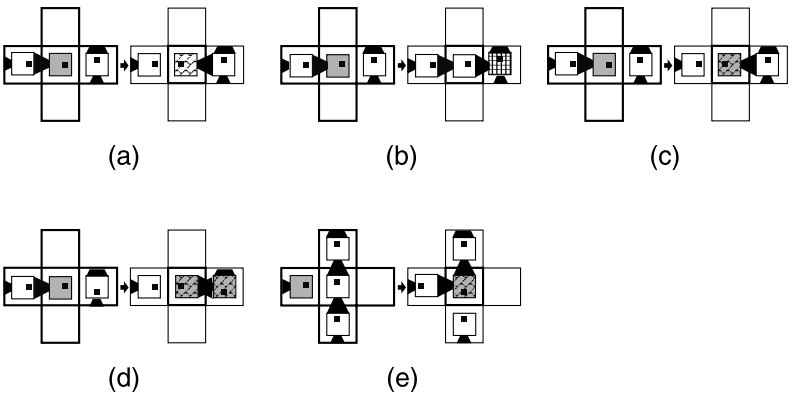

Figure 28.

A2.3 Interaction Rule for All `structure` Cells

When the center cell is in any mode other than DESTROY or WITHDRAW, and any of its neighbors is in DECODE mode with its `gene` field directed toward the center cell, then, depending on the interaction type, one of the following transition rules (Figure 29) is applied:

(a) Defensive (non-left-side): If the `structure` cell is not the front left neighbor of the center cell, the `gene` field of the rear neighbor is copied to the `gene` field of the center cell.

(b) Defensive (left-side): In other cases, the transition rule for the single loop is applied.

(c) Counter: The `gene` field of the rear neighbor is copied to the center cell.

(d) Cancel, (e) inroad: The `gene` field of the center cell is redirected to line up with its `link` field, after which the `link` field is redirected to point to the DECODE-mode cell. The center cell switches to DESTROY mode.

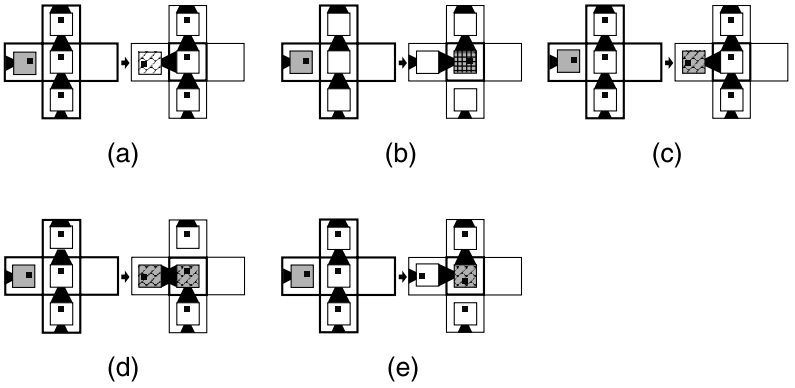

Figure 29.

This article has been cited by:

1. Takashi Ikegami. 2010. Chemical Robot: Self-organizing Self-moving Oil Droplet. *Journal of the Robotics Society of Japan* **28**:4, 435-444. [CrossRef]
2. Takashi Ikegami, Martin M Hanczyc. 2009. The search for a first cell under the maximalism design principle. *Technoetic Arts: a Journal of Speculative Research* **7**:2, 153-164. [CrossRef]
3. Hiroki Sayama. 2008. Construction theory, self-replication, and the halting problem. *Complexity* **13**:5, 16-22. [CrossRef]